


RESEARCH ARTICLE

# Pathology-specific patterns of cerebellar atrophy in neurodegenerative disorders

Yu Chen<sup>1</sup>  | Salvatore Spina<sup>1</sup> | Patrick Callahan<sup>1</sup> | Lea T. Grinberg<sup>1,2</sup> | William W. Seeley<sup>1,2</sup> | Howard J. Rosen<sup>1</sup> | Joel H. Kramer<sup>1</sup> | Bruce L. Miller<sup>1</sup> | Katherine P. Rankin<sup>1</sup>

<sup>1</sup>Department of Neurology, Memory and Aging Center, Weill Institute for Neurosciences, University of California San Francisco, San Francisco, California, USA

<sup>2</sup>Department of Pathology, University of California San Francisco, San Francisco, California, USA

## Correspondence

Yu Chen, Memory and Aging Center, Department of Neurology, University of California San Francisco, 1651 4th Street, San Francisco, CA 94158, USA.  
Email: [SherryYu.Chen@ucsf.edu](mailto:SherryYu.Chen@ucsf.edu)

## Funding information

National Institutes of Health, Grant/Award Numbers: P01AG019724, P50AG023501, P30AG062422, U01AG057195, U19AG063911, U01AG045390, U54NS092089, R01AG029577; Larry L. Hillblom Foundation, Grant/Award Number: 2014-A-004-NET; Rainwater Charitable Foundation; Bluefield Project to Cure FTD

[Correction added on January 8, 2024, after first online publication: The funding information has been updated.]

## Abstract

**INTRODUCTION:** Associations of cerebellar atrophy with specific neuropathologies in Alzheimer's disease and related dementias (ADRD) have not been systematically analyzed. This study examined cerebellar gray matter volume across major pathological subtypes of ADRD.

**METHODS:** Cerebellar gray matter volume was examined using voxel-based morphometry in 309 autopsy-proven ADRD cases and 80 healthy controls. ADRD subtypes included AD, mixed Lewy body disease and AD (LBD-AD), and frontotemporal lobar degeneration (FTLD). Clinical function was assessed using the Clinical Dementia Rating (CDR) scale.

**RESULTS:** Distinct patterns of cerebellar atrophy were observed in all ADRD subtypes. Significant cerebellar gray matter changes appeared in the early stages of most subtypes and the very early stages of AD, LBD-AD, FTLD-TDP type A, and progressive supranuclear palsy. Cortical atrophy positively predicted cerebellar atrophy across all subtypes.

**DISCUSSION:** Our findings establish pathology-specific profiles of cerebellar atrophy in ADRD and propose cerebellar neuroimaging as a non-invasive biomarker for differential diagnosis and disease monitoring.

## KEYWORDS

Alzheimer's disease, cerebellum, frontotemporal lobar degeneration, Lewy body disease, neuroimaging, neuropathology, tau, TDP-43

## Highlights

- Cerebellar atrophy was examined in 309 patients with autopsy-proven neurodegeneration.
- Distinct patterns of cerebellar atrophy are found in all pathological subtypes of Alzheimer's disease and related dementias (ADRD).

This is an open access article under the terms of the [Creative Commons Attribution-NonCommercial](https://creativecommons.org/licenses/by-nc/4.0/) License, which permits use, distribution and reproduction in any medium, provided the original work is properly cited and is not used for commercial purposes.

© 2023 The Authors. *Alzheimer's & Dementia* published by Wiley Periodicals LLC on behalf of Alzheimer's Association.

- Cerebellar atrophy is seen in early-stage (Clinical Dementia Rating [CDR]  $\leq 1$ ) AD, Lewy body dementia (LBD), frontotemporal lobar degeneration with tau-positive inclusion (FTLD-tau), and FTLD-transactive response DNA binding protein (FTLD-TDP).
- Cortical atrophy positively predicts cerebellar atrophy across all neuropathologies.

## 1 | BACKGROUND

Alzheimer's disease (AD), diffuse neocortical Lewy body disease (LBD), and frontotemporal lobar degeneration (FTLD) are the most common neurodegenerative disorders leading to dementia.<sup>1-4</sup> Patients with these disorders frequently present with overlapping symptoms, such as multi-domain cognitive deficits, behavioral changes, and movement dysfunction. Although a substantial body of work has been conducted to describe patterns of regional cerebral changes that are associated with these disorders, as well as the brain-behavior relationships underlying specific dementia symptoms, much less attention has been paid to the contributions of the cerebellum. Indeed,  $\approx 80\%$  of all neurons in the human brain are located in the cerebellum.<sup>5</sup> Preliminary studies suggest that the cerebellum is differentially affected in various neurodegenerative disorders<sup>6,7</sup> and is associated with their clinical presentations<sup>8-10</sup>; however, the pattern and extent of cerebellar structural changes in relation to the specific pathologies remain understudied.

Neuropathological confirmation is the gold standard for identifying the underlying dementia syndromes; however, syndrome-pathology relationships are complex. The pathology underlying frontotemporal dementia (FTD) syndromes, for example, is heterogeneous and is not limited to FTLD. The pathologic consensus criteria proposed in 2010 classified FTLD into three major pathological subgroups: FTLD with tau-positive inclusion (FTLD-tau), FTLD with ubiquitin-positive and transactive response DNA binding protein of 43 kDa (TDP-43)-positive, but tau-negative inclusions (FTLD-TDP), and FTLD with the fused in sarcoma (FUS) protein-positive but tau-negative and TDP-43-negative inclusions (FTLD-FUS).<sup>11</sup> In addition, a small number of FTLD cases with ubiquitin-positive, but tau-, TDP-43, and FUS-negative inclusions are classified as FTLD-UPS. Based on the pathological changes, the distribution of these changes, and the associated genetic defects, TDP-43-positive cases can be divided further into five types (A-E).<sup>12,13</sup> It should be noted that patients with a clinical diagnosis of FTD can also have a primary pathological diagnosis of AD.<sup>14,15</sup> Furthermore, distinct neuropathologies often co-occur.<sup>16,17</sup>

Despite the importance of using neuropathology to define disease, previous imaging studies investigating cerebellar contributions in dementia have been based on clinical rather than pathological diagnosis.<sup>6</sup> Our previous work in the subtypes of FTD syndrome has suggested that pathology is likely another relevant variable when investigating cerebellar contributions to cognitive dysfunction.<sup>18</sup> Careful separation of patients with dementia into pathologically homogeneous groups could provide important insight into the cerebellar biology of each disease and help to further define neuroanatomic

correlations with clinical features and causative mutations. Distinct patterns of whole-brain atrophy have been described in different pathological subtypes of dementia,<sup>19,20</sup> leading to questions about whether the patterns of cerebellar atrophy may differ, whether they could be detected in the early stage of the disease, and what the relationship is between cerebellar and cerebral atrophy in these diseases. The large effect sizes of localized cerebral atrophy in a whole-brain analysis, however, affect the statistical thresholds in a manner that biases the detection of significant voxels toward cerebral regions, washing out potentially significant associations in the cerebellum. To fill these gaps, we used voxel-based morphometry (VBM) analysis within a cerebellar region of interest (ROI) to identify patterns of cerebellar atrophy in the major pathological subtypes of amnesic AD, dementia with Lewy bodies (DLB), and FTD, and then showed the associations of these cerebellar patterns with cerebral atrophy. In light of the existing literature, we predicted that (1) distinct patterns of regional cerebellar atrophy would be found in different pathologically defined patient groups; (2) cerebellar atrophy could be found even in the early stage of the disease; and (3) the degree of cerebellar atrophy would be associated with the degree of cerebral atrophy in all pathological subtypes.

## 2 | METHODS

### 2.1 | Participants

A total of 309 patients with dementia were included through the Memory and Aging Center (MAC) at the University of California, San Francisco (UCSF). All patients had undergone postmortem examination and had structural magnetic resonance imaging (MRI) brain scans. The pathological diagnosis was made based on current consensus criteria including FTLD ( $n = 158$ ),<sup>11,12</sup> AD ( $n = 77$ ),<sup>21</sup> and LBD ( $n = 74$ ).<sup>22</sup> The AD group consisted of 76 cases with AD neuropathological change equal to or higher than intermediate.<sup>23</sup> One case had low AD neuropathological change (A1, B2, C0) with Braak neurofibrillary tangle stage 4.<sup>23,24</sup>

We included cases with a single primary pathology (i.e., a single pathological entity with severity and topographical distribution of findings that are sufficient to explain the majority of the symptoms experienced by the patient), and excluded those with comorbid primary pathologies, while retaining cases with contributing or incidental copathologies.<sup>17</sup> The AD group consisted of patients with only AD pathology, in the absence of LBD or FTLD copathologies. Limbic argyrophilic grain disease was allowed. Because our brain bank lacks a

significant representation of pure LBD cases free of AD pathology, our LBD group ( $n = 74$ ) consisted of patients who also had some degree of coexisting AD neuropathological changes (LBD-AD). Twenty-six had diffuse neocortical LBD, 17 patients had limbic-transitional LBD, 4 patients had brainstem-only LBD, and 27 patients had amygdala-predominant LBD. Patients with FTLN were further classified into FTLN major molecular classes and subtypes: FTLN-TDP (FTLN-TDP type A [TDP-A;  $n = 21$ ], FTLN-TDP type B [TDP-B;  $n = 21$ ], FTLN-TDP type C [TDP-C;  $n = 26$ ], and FTLN-tau Pick's disease [ $n = 25$ ], corticobasal degeneration [CBD;  $n = 32$ ], and progressive supranuclear palsy [PSP;  $n = 33$ ]). Of note, the TDP-A group also included cases with hippocampal sclerosis. The TDP-B group included cases with or without motor neuron disease, as well as cases with comorbid atypical tauopathy. The TDP-C group included two cases with comorbid motor neuron disease. Low AD neuropathologic changes (110/158), and brainstem-only (19/158) or amygdala-predominant LBD pathology (2/158) were allowed in the FTLN groups. Cases with other primary pathological diagnoses (e.g., cerebrovascular disease, unclassifiable FTLN-TDP, unclassifiable FTLN-tau, FTLN due to microtubule-associated protein tau pathogenic variants (FTLN-MAPT), FTLN-FUS, atypical FTLN with ubiquitinated inclusions (FTLN-U), argyrophilic grain disease, Huntington's disease, Parkinson's disease, and globular glial tauopathies type I) were not included in the study because the numbers were insufficient to support group analyses. We also identified the clinical diagnosis of patients, which had been determined during life by an expert multidisciplinary team of neurologists, neuropsychologists, and nurses according to current clinical diagnostic criteria.<sup>25-33</sup>

The level of clinical functioning at the time of the structural MRI scan was assessed with the Clinical Dementia Rating (CDR) scale<sup>34,35</sup> and/or Clinical Dementia Rating Scale plus National Alzheimer's Coordinating Center Behavior and Language Domains (FTLN-CDR),<sup>36</sup> with the global score ranging from 0 (normal), 0.5 (very mildly impaired), 1 (mildly impaired), 2 (moderately impaired), to 3 (severely impaired). The FTLN-CDR includes the two additional behavior and language domains that are predominantly affected in FTLN, and, therefore, enhances the utility of the CDR in FTLN spectrum. In addition, 80 healthy adults were included as controls.

The study was approved by the UCSF Committee on Human Research. All participants were recruited at the MAC of UCSF and provided written informed consent or assent in accordance with the Declaration of Helsinki. This study was performed in accordance with the ethical standards as laid down in the 1964 Declaration of Helsinki and its later amendments or comparable ethical standards.

## 2.2 | Neuropathology

Pathological diagnosis was assessed for each case with autopsy. Neuropathological assessments were performed at UCSF according to published procedures and diagnoses were rendered according to published criteria.<sup>37-39</sup>

## RESEARCH IN CONTEXT

- 1. Systematic review:** The authors reviewed studies on cerebellar involvement in neurodegenerative disorders and the syndrome-pathology relations underlying dementia syndromes using PubMed. Previous studies, primarily based on clinical diagnosis, suggest that cerebellar involvement varies across disorders and is associated with clinical presentations. The cerebellar structural changes specific to different pathologies remain understudied.
- 2. Interpretation:** Our findings reveal distinct patterns of cerebellar atrophy in Alzheimer's disease (AD) and related dementias (ADRD) including AD, mixed Lewy body disease and AD, and frontotemporal lobar degeneration, even in the early stages. Cerebellar atrophy seems to directly reflect the degree of cerebral atrophy, regardless of neuropathology.
- 3. Future directions:** These findings suggest the potential for cerebellar neuroimaging as a non-invasive biomarker for differential diagnosis and monitoring. Clarification of cerebellar involvement throughout disease progression and longitudinal and individual studies examining pathological burden and its association with cerebellar volume loss are needed. Functional network studies will also help understand the mechanisms behind these anatomic changes.

## 2.3 | MRI acquisition and preprocessing

All participants underwent whole-brain structural MRI with 3T (252 cases), 1.5T (90 cases), or 4T (47 cases) with published acquisition parameters.<sup>40-42</sup> In patients with multiple MRI scans, only the earliest scan was included in this study.

Three-dimensional (3D) T1-weighted images were preprocessed using Statistical Parametric Mapping 12 (SPM; <https://www.fil.ion.ucl.ac.uk/spm>). The images were inspected visually for artifacts and underwent bias correction. Brain-extracted images were then segmented into tissue compartments (gray matter, white matter, and cerebrospinal fluid) and spatially normalized to the Montreal Neurological Institute standard space (MNI152) using a single generative model with the default tissue probability maps from SPM12 (TPM.nii). A template of older adults was generated from 300 confirmed neurologically healthy older adults (ages 44-86 years, mean  $\pm$  SD: 67.2  $\pm$  7.3; 114 male, 186 female). To optimize inter-participant registration, each image was concatenated into this template with affine and non-linear transformation using the diffeomorphic anatomic registration through exponentiated lie algebra (DARTEL) tools. The resulting spatially normalized, segmented, and modulated gray matter images were then smoothed with an 8-mm full-width half-maximum (FWHM) isotropic

Gaussian kernel. In all preprocessing steps, default parameters of the SPM12 toolbox were used. The total intracranial volume (TIV) for each individual was derived by summing the total volume of gray matter, white matter, and cerebrospinal fluid. An ROI mask of the cerebellum was created based on the Cerebellar Atlas in MNI152 space after normalization with FMRIB Nonlinear Registration Tool (FNIRT).<sup>43,44</sup> This cerebellum mask was used in subsequent analyses.

## 2.4 | Voxel-based morphometry analyses

VBM analyses were conducted on the 3D T1-weighted sequences using the FMRIB Software Library (FSL) package version 6.0.5 (<https://fsl.fmrib.ox.ac.uk/fsl>). Atrophy analyses were performed to investigate between-group differences of gray matter volume. Voxel-wise general models were applied using permutation-based non-parametric testing<sup>45</sup> with 5000 permutations per contrast. Age, sex, TIV, and magnet strength were entered as covariates in these models. Whole-brain VBM analyses between patient groups and controls were first carried out to determine the patterns of brain atrophy specific to each pathological subtype. Differences of cerebellar gray matter volume were then assessed between patients and controls with the ROI mask of the cerebellum. In addition, pairwise group contrasts were conducted between patient groups and controls separately for CDR 0–0.5 and CDR  $\leq 1$  to investigate atrophy patterns in the earlier clinical stages.

Significant clusters were identified by employing the voxel-based method with a threshold of  $p < 0.05$  corrected for family-wise error (FWE). Results are reported with a cluster extent threshold of 100 contiguous voxels. Imaging results of cerebellar atrophy were overlaid on cerebellar surface-based flatmaps provided by SUIT toolbox<sup>46</sup> based on Matlab, version R2021a (<https://www.mathworks.com/products/matlab.html>) and SPM12.

## 2.5 | Relationship of cerebral to cerebellar volume

Individual-level sum intensity values were extracted from the significant clusters of both cerebral and cerebellar atrophy from the VBM analyses. We performed linear regression analyses to explore whether the cerebellar intensity values were significantly predicted by the cerebral intensity values, and we repeated this step by controlling for age, sex, and TIV. R values of the correlations between patient groups and controls were compared using the cocor package<sup>47</sup> of RStudio 2021.09.0 (<https://www.rstudio.com>). Finally, we conducted a slope difference test to examine whether the slopes of the regressions differed between patient groups and controls.<sup>48,49</sup>

## 2.6 | Additional statistical analyses

Statistical analyses were conducted using RStudio 2021.09.0. Demographic (age and education) and clinical (CDR, FTLD-CDR) variables

were examined across groups via analysis of variance (ANOVA) with *post hoc* comparison using the Dunnett-Hsu test. Sex was compared by chi-square. A significance level of  $p < 0.05$  was considered statistically significant.

## 3 | RESULTS

### 3.1 | Demographics and clinical characteristics

Group differences were present for age ( $F(8, 380) = 2.8, p = 0.005$ ) and sex ( $\chi^2(8, 389) = 25.9, p = 0.001$ ) (Table 1). No statistically significant group differences were found for education ( $F(9, 369) = 0.5, p = 0.87$ ). Therefore, only age and sex were included as confounding covariates to be controlled for all imaging and statistical analyses. As expected, patient groups scored significantly worse on CDR ( $F(8, 340) = 30.6, p < 0.001$ ) and FTLD-CDR ( $F(8, 290) = 38.8, p < 0.001$ ) compared with the healthy controls.

### 3.2 | Clinicopathologic correlations

The association between pathological subtype and atrophy could be influenced by the proportion of individuals in the group with particular clinical syndromes; thus we identified the clinical presentations of the cases within each pathological group (Table 1). The most predominant clinical syndromes in each group are as follows. In the TDP-A group, 15 (71.4%) were diagnosed with behavioral variant frontotemporal dementia (bvFTD). In the TDP-B group, 9 patients (42.9%) were diagnosed with bvFTD. In the TDP-C group, 24 patients (92.3%) were diagnosed with semantic variant primary progressive aphasia (svPPA). In the Pick's disease group, 13 patients (52.0%) were diagnosed with bvFTD. In the

CBD group, 13 patients (40.6%) were diagnosed with corticobasal syndrome (CBS). In the PSP group, 25 patients (75.8%) were diagnosed with PSP syndrome. In the AD group, 60 patients (77.9%) were diagnosed with amnesic AD or mild cognitive impairment (MCI) syndrome, and 3 had atypical AD syndromes. Co-existing AD pathology was observed in all patients with LBD. In the LBD-AD group, 58 patients (78.4%) were diagnosed with AD syndrome.

### 3.3 | VBM results

#### 3.3.1 | Pattern of cerebellar atrophy

Comparisons against controls were carried out for each pathological group with an ROI mask of the cerebellum (Figure 1, Table 2). In addition, pairwise group contrasts were performed between controls and patient groups for CDR 0–0.5 and CDR  $\leq 1$  separately to investigate cerebellar atrophy in the earlier clinical stages (Figure 2).

**TABLE 1** Demographic information and score results of the participants (n = 389).

M (SD)	Control (n = 80)	TDP-A (n = 21)	TDP-B (n = 21)	TDP-C (n = 26)	Pick's (n = 25)	CBD (n = 32)	PSP (n = 33)	AD (n = 77)	LBD-AD (n = 74)	F (df)	p	$\eta^2$
Age at Scan (y)	65.8 (8.9)	62.8 (5.1)	58.1 <sup>†</sup> (8.6)	63.3 (7.3)	62.3 (6.5)	64.5 (6.2)	68.6 (7.2)	64.4 (10.7)	64.7 (10.3)	2.8 (8)	0.005	0.06
Time From Scan to Death (y)	-	4.5 (3.5)	2.2 (2.7)	7.8 (2.7)	5.6 (3.0)	2.6 (1.6)	3.0 (1.9)	5.7 (3.4)	5.5 (3.1)	12.6 (7)	<0.001	0.23
Sex(M/F)	25/55	8/13	10/11	12/14	15/10	15/17	16/17	38/39	52/22	25.9 <sup>†</sup> (8)	0.001	0.53
Education	16.5 (2.8)	15.6 (3.5)	16.0 (3.3)	17.0 (2.8)	15.9 (2.0)	16.6 (3.0)	16.3 (3.9)	16.6 (3.5)	16.7 (3.4)	0.5 (8)	0.872	0.01
CDR	0.0 (0.0)	1.1 <sup>***</sup> (0.8)	1.6 <sup>***</sup> (0.9)	0.78 <sup>***</sup> (0.6)	0.9 <sup>***</sup> (0.6)	0.8 <sup>***</sup> (0.6)	0.7 <sup>***</sup> (0.4)	0.9 <sup>***</sup> (0.5)	0.9 <sup>***</sup> (0.5)	30.6 (8)	<0.001	0.42
FTLD-CDR	0.0 (0.0)	1.5 <sup>***</sup> (0.9)	1.7 <sup>***</sup> (0.8)	1.2 <sup>***</sup> (0.7)	1.4 <sup>***</sup> (0.7)	1.2 <sup>***</sup> (0.7)	1.1 <sup>***</sup> (0.6)	1.1 <sup>***</sup> (0.5)	1.2 <sup>***</sup> (0.6)	38.8 (8)	<0.001	0.52
FTLD-CDR Box Score	0.0 (0.0)	8.5 <sup>***</sup> (3.3)	11.2 <sup>***</sup> (5.7)	6.9 <sup>***</sup> (3.9)	7.0 <sup>***</sup> (3.3)	6.3 <sup>***</sup> (4.8)	5.5 <sup>***</sup> (3.4)	5.8 <sup>***</sup> (3.4)	7.2 <sup>***</sup> (3.5)	35.3 (8)	<0.001	0.49
Clinical Presentation												
bvFTD	0	15	9	1	13	8	0	0	1			
FTD-ALS	0	0	8	0	0	0	0	1	1			
svPPA	0	1	2	24	1	0	0	0	1			
nvPPA	0	3	1	0	8	6	3	3	0			
CBS	0	1	0	0	2	13	2	6	2			
PSP	0	0	0	0	0	3	25	0	1			
CBS/PSP	0	1	0	0	0	1	1	0	1			
AD	0	0	0	0	1	0	0	53	58			
AD/CBS	0	0	0	0	0	0	0	1	0			
DLB	0	0	0	0	0	0	0	0	3			
AD/DLB	0	0	0	0	0	0	0	0	2			
lvPPA	0	0	0	0	0	0	0	2	0			
PSYCH	0	0	0	0	0	1	0	0	0			
Prion	0	0	0	0	0	0	0	1	0			
MCI	0	0	1	1	0	0	1	7	3			
Normal	80	0	0	0	0	0	0	3	1			

Notes: Values are mean with SD in brackets. Bold numbers indicate the most common associated pathologies underlying clinical diagnoses.

Abbreviations: AD, Alzheimer's disease; ALS, amyotrophic lateral sclerosis; bvFTD, behavioral variant frontotemporal dementia; CBD, corticobasal degeneration; CBS, corticobasal syndrome; CDR, Clinical Dementia Rating; DLB, dementia with Lewy body disease; FTLD-CDR, CDR Dementia Staging Instrument PLUS National Alzheimer's Coordinating Center (NACC) Behavior and Language Domains; LBD, Lewy body disease; lvPPA, logopenic variant primary progressive aphasia; MCI, mild cognitive impairment; nvPPA, nonfluent variant primary progressive aphasia; PSP, progressive supranuclear palsy; PSYCH, psychiatric disorders (i.e., bipolar disorder, late-life psychiatric, major depressive disorder); svPPA, semantic variant primary progressive aphasia; TDP, transactive response DNA binding protein.

<sup>†</sup> Chi-square value.

\*, \*\*\*, Group differs from control group at \*p < 0.05, \*\*\*p < 0.001.

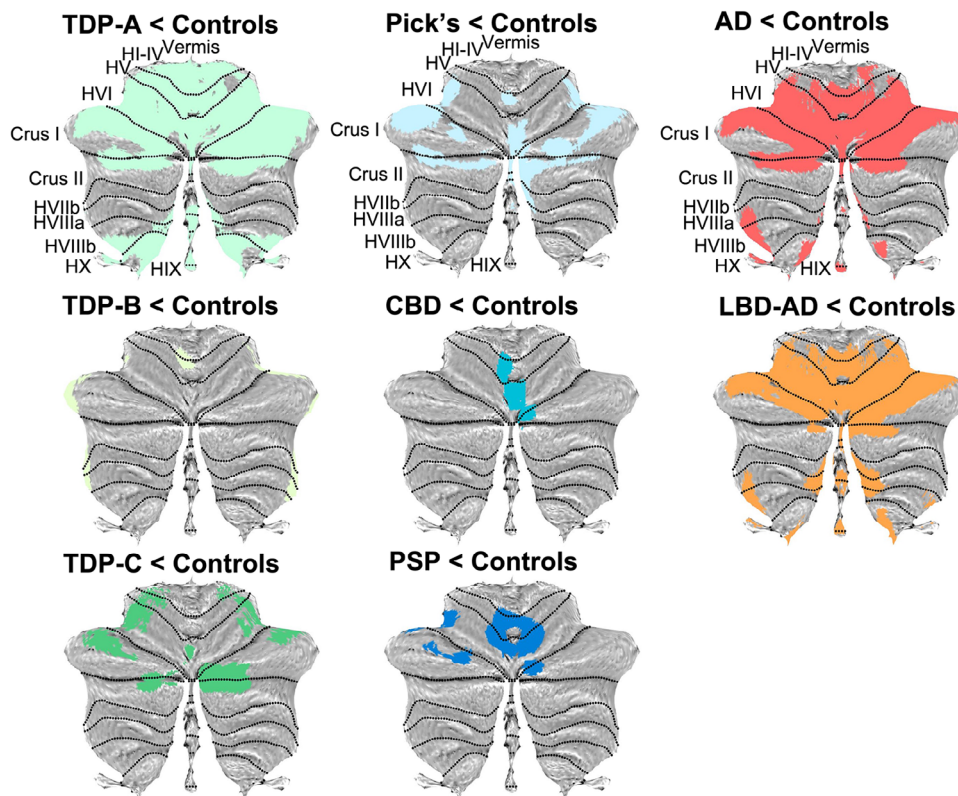


**FIGURE 1** Voxel-based morphometry analyses showing regions of decreased cerebellar gray matter density in contrasts between patient groups and controls. Each pathological subtype is coded with a distinct color. Colored voxels show regions that were significant in the analyses at the threshold of  $p < 0.05$  corrected for family-wise error with a cluster threshold of 100 contiguous voxels. AD, Alzheimer's disease; CBD, corticobasal degeneration; LBD, Lewy body disease; PSP, progressive supranuclear palsy.

#### *FTLD < controls*

Compared with controls, cerebellar atrophy was found in all FTLD subgroups involving the bilateral hemispheres and the vermis.

#### *FTLD-TDP < controls*

In TDP-A, widespread cerebellar atrophy was observed bilaterally affecting lobules I–VI, Crus I, Crus II, lobules VIIb, VIIIa, VIIIb, IX, and X, as well as the vermis. At CDR 0–0.5 ( $n = 8$ ), only the left lobule VI was affected. At CDR  $\leq 1$  ( $n = 12$ ), the reduced gray matter intensity was present bilaterally in lobules I–V, IX, left lobule VI, and Crus I.

In TDP-B, cerebellar atrophy was observed bilaterally in lobules V–VI, Crus I, Crus II, VIIb, VIIIa, left I–IV, and right lobule VIIIb. No significant cerebellar atrophy was found at CDR 0–0.5 ( $n = 4$ ) or  $\leq 1$  ( $n = 10$ ).

In TDP-C, cerebellar atrophy was observed bilaterally in lobules I–VI, Crus I, Crus II, and the vermis. At CDR  $\leq 1$  ( $n = 19$ ), significant cerebellar atrophy was observed bilaterally in lobules V, VI, Crus I, and right Crus II. No significant cerebellar atrophy was found at CDR 0–0.5 ( $n = 15$ ).

#### *FTLD-tau < controls*

In Pick's disease, cerebellar atrophy was observed bilaterally in lobules V, VI, Crus I, Crus II, right lobules VIIb, VIIIa, and the vermis. At CDR  $\leq 1$  ( $n = 21$ ), cerebellar atrophy was found bilaterally in lobules VI,

Crus I, Crus II, right lobules VIIb, VIIIa, and the vermis. No significant cerebellar atrophy was found at CDR 0–0.5 ( $n = 9$ ).

In CBD, cerebellar atrophy was observed in bilateral lobules V, VI, left lobules I–IV, right Crus I, and the vermis. At CDR  $\leq 1$  ( $n = 28$ ), focal cerebellar atrophy was found in the left lobules I–VI, bilateral Crus I, and the vermis. No significant cerebellar atrophy was found at CDR 0–0.5 ( $n = 15$ ).

In PSP, cerebellar atrophy was found bilaterally affecting lobules I–VI, Crus I, and the vermis. At CDR 0–0.5 ( $n = 19$ ), cerebellar atrophy was present bilaterally in lobules I–VI, Crus I, left Crus II, and the vermis. At CDR  $\leq 1$  ( $n = 27$ ), atrophy extended more posterior affecting the right Crus II.

#### *AD < controls*

Compared with controls, widespread reduction in cerebellar gray matter intensity was found in all cerebellar lobules and the vermis in AD. At CDR 0–0.5 ( $n = 31$ ), only bilateral Crus I and right lobule VI were affected. At CDR  $\leq 1$  ( $n = 50$ ), widespread cerebellar atrophy was found involving bilateral lobules I–VI, Crus I, lobule IX, left lobules VIIIa, VIIIb, and the vermis.

#### *LBD-AD < controls*

In LBD-AD, widespread cerebellar atrophy was found in all cerebellar lobules and the vermis. At CDR 0–0.5 ( $n = 24$ ), focal cerebellar atrophy

**TABLE 2** Voxel-based morphometry results of significant cerebellar gray matter density decrease between patient groups and controls.

Contrast	Cluster size (voxels)	MNI coordinates			T value	Hemisphere	Regions
		x	y	z			
TDP-A < Controls	13225	-54	-53	-32	3.664	Bilateral	Left Crus I extending into bilateral lobules I-VI, Crus I, Crus II Vermis
	3623	-5	-57	-65	3.664	Bilateral	Left lobule IX extending into bilateral VIIB, VIIIA, VIIIB, IX, X Vermis
TDP-B < Controls	514	-44	-41	-45	3.458	Left	Left Crus II extending into lobule VI, Crus I, lobules VIIb, VIIIA
	395	38	-39	-47	3.458	Right	Lobule VIIIA extending into Crus I, Crus II, lobule VIIb, VIIIB
	207	-8	-56	-3	3.334	Left	Lobule V extending into lobule I-IV
	137	47	-45	-29	2.470	Right	Crus I extending into lobules V, VI
TDP-C < Controls	1240	21	-89	-27	3.658	Right	Crus I extending into lobule VI, Crus II
	743	-41	-39	-32	3.658	Left	Lobule VI extending into lobules I-V, Crus I
	566	-33	-83	-36	2.841	Left	Crus I extending into lobule VI, Crus II Vermis
	459	44	-38	-33	3.658	Right	Lobule VI extending into lobules I-V, Crus I
Pick's < Controls	3373	45	-39	-32	3.659	Bilateral	Right Crus I extending into bilateral Crus I, Crus II, right lobules V, VI, VIIb, VIIIA
						Vermis	
	740	-50	-45	-33	3.659	Left	Crus I extending into lobules V, VI
	170	-3	-62	-3	3.170	Bilateral	Left lobule V extending into bilateral lobules V and left lobules I-IV
	125	-38	-78	-24	2.297	Left	Crus I
CBD < Controls	920	-2	-75	-14	3.081	Bilateral	Vermis extending into bilateral lobules V, VI, left lobules I-IV, right Crus I
						Vermis	
PSP < Controls	1325	12	-68	-12	3.447	Bilateral	Right lobule VI extending into bilateral lobules I-VI
						Vermis	
	183	-36	-78	-23	2.486	Left	Crus I extending into Crus II
	117	-39	-48	-27	2.507	Left	Lobule VI extending into Crus I
	112	14	-83	-20	2.380	Right	Crus I extending into lobule VI
AD < Controls	10154	-26	-41	-57	3.618	Bilateral	Left VIIIB extending into bilateral lobules I-VI, Crus I, Crus II, left lobules VIIIA, VIIIB, IX, X
						Vermis	
	887	0	-57	-60	3.212	Bilateral	Right lobule IX extending into bilateral lobules VIIb, VIIIA, IX, right lobule VIIIB
						Vermis	
	144	-5	-47	-33	3.037	Bilateral	Vermis extending into bilateral lobules IX
					Vermis		
	139	24	-36	-52.5	2.823	Right	Lobule VIIIB extending into lobule X
LBD- AD < Controls	9612	3	-75	-47	3.620	Bilateral	Right lobule VIIb extending into bilateral lobules I-VI, Crus I, Crus II, VIIb, VIIIA, VIIIB, right lobules IX, X
						Vermis	
	609	0	-48	-45	2.995	Bilateral	Right lobule IX extending into left lobule IX
					Vermis		
	513	-29	-39	-56	3.620	Left	Lobule VIIIB extending into lobules VIIIA, X

Note: Clusters were thresholded at  $p < 0.05$  corrected for family-wise error with a cluster extent threshold of 100 contiguous voxels.

Abbreviations: AD, Alzheimer's disease; CBD, corticobasal degeneration; LBD, Lewy body disease; PSP, progressive supranuclear palsy.

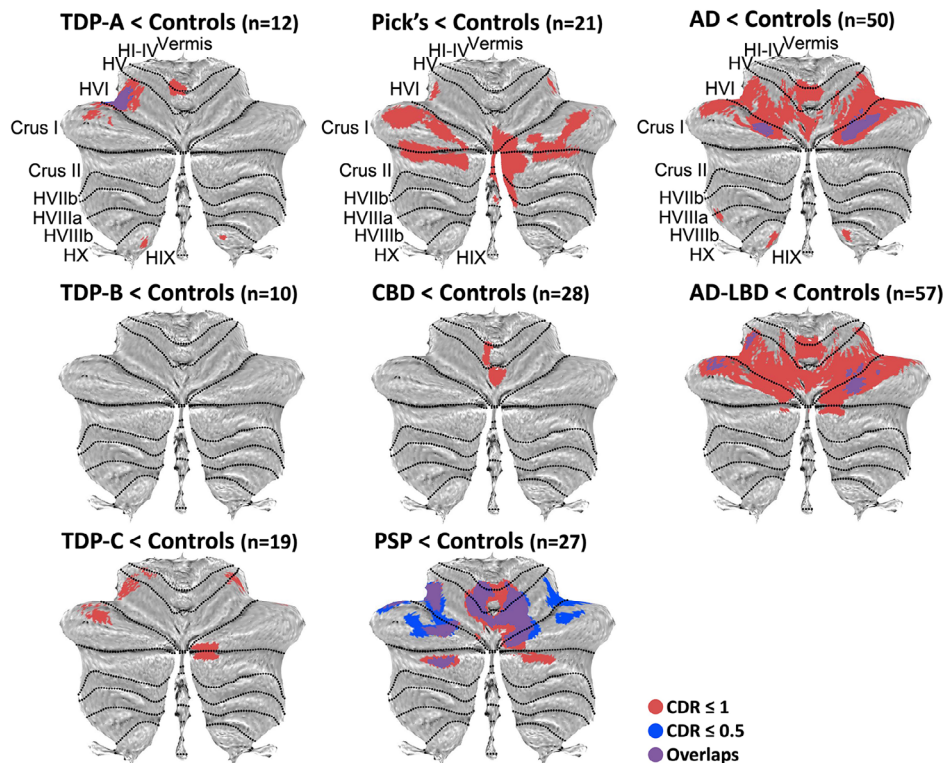


**FIGURE 2** Voxel-based morphometry analyses showing regions of decreased cerebellar gray matter density in contrasts between patient groups and controls at CDR stages 0–0.5 (navy), and  $\leq 1$  (red). Colored voxels show regions that were significant in the analyses at the threshold of  $p < 0.05$  corrected for family-wise error with a cluster threshold of 100 contiguous voxels. AD, Alzheimer's disease; CBD, corticobasal degeneration; CDR, Clinical Dementia Rating; LBD, Lewy body disease; PSP, progressive supranuclear palsy.

was found in bilateral lobules VI and Crus I. At CDR  $\leq 1$  ( $n = 57$ ), cerebellar atrophy was observed involving the lobules I–VI, Crus I, Crus II, bilaterally, and the vermis.

### 3.3.2 | Pattern of whole-brain atrophy

Whole-brain VBM analyses revealed the canonical patterns of atrophy specific to each pathological subtype (Figures S1 and S2).

### 3.4 | Relationship between cerebral and cerebellar volume

We also performed an exploratory analysis to identify whether cerebellar atrophy can be predicted by cerebral atrophy in each pathological subgroup (Figure 3), as represented by voxel intensity values. Linear regression analyses revealed that cerebellar volume was predicted by the cerebral volume in all pathological subgroups (all  $p < .05$ ) when controlling for age, sex, and TIV. In addition, we further explored the differences of the  $r$  values of the correlations and the regression slopes between patient groups and controls. A significant group difference was found for the regression slope in LBD-AD compared with controls, with LBD-AD showing a less steep slope than the controls, suggesting greater cerebellar atrophy than predicted.

## 4 | DISCUSSION

This study established for the first time the patterns of cerebellar gray matter changes in autopsy-confirmed neurodegenerative diseases. Cerebellar atrophy is observed in all pathologies, and the cerebellum is differentially affected, even in the earlier stage of the disease before functional deficits consistent with dementia are present. These cerebellar changes are highly correlated with the extent of cerebral gray matter changes. These results indicate that the pathology-specific involvement of the cerebellum in dementia may be more pronounced earlier than previously thought.

All patient groups showed cerebellar atrophy localized bilaterally in cerebellar hemispheres. Cerebellar atrophy was particularly widespread in AD, LBD-AD, and TDP-A, with all cerebellar lobules and the vermis affected. This contrasted with the comparatively focal atrophy found in other pathologies. Because our sample of LBD consistently had AD co-pathology, the pattern of cerebellar atrophy in LBD-AD may have been driven predominantly by AD. Atrophy patterns of the pathologies were broadly in line with the combined patterns of their most common associated clinical syndromes (Table 1).<sup>10,50,51</sup>

It is important to note that these cerebellar atrophy patterns appear to dovetail with characteristic symptoms in these diseases. For example, the cerebellar regions involved in AD and LBD-AD are connected with memory-specific structures in the cerebrum. Specifically, cerebellar lobules VIIb and IX are a part of the default mode network<sup>52,53</sup>;



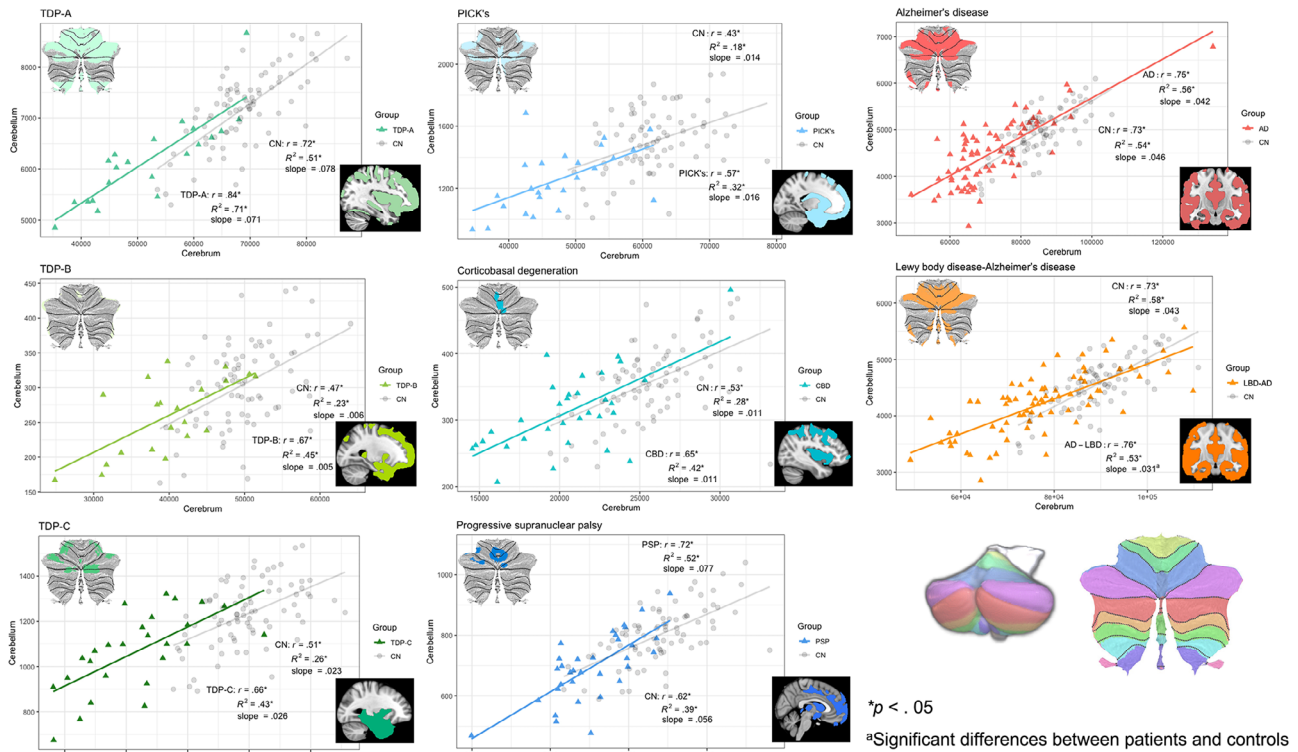


**FIGURE 3** Relationship between cerebellar and cerebral intensity values of the significant clusters from the VBM analyses. Each pathological subtype is coded with a distinct color. AD, Alzheimer's disease; CBD, corticobasal degeneration; LBD, Lewy body disease; PSP, progressive supranuclear palsy; VBM, voxel-based morphometry.

lobules I–V, VIIIa, and IX connect to the hippocampus<sup>53</sup>; and Crus I and II<sup>54</sup> have been associated with episodic and working memory decline in AD.<sup>9</sup> Crus II; lobules VI, VIIb, VIIIa; and the vermis involved in LBD-AD, Pick's, TDP-A, and TDP-B have been associated with neuropsychiatric deficits in patients with DLB and bvFTD.<sup>54–56</sup> Crus I, Crus II, lobules VI, VIIb, and IX impacted in Pick's, TDP-A, and TDP-B are connected with the adaptive executive network in the cerebrum, and have been associated with deficits in executive function in FTD.<sup>18,52</sup> Crus I, Crus II, lobules I–VI, and VIIb affected in Pick's, TDP-A, and TDP-B are connected with the cerebral salience network, which has been associated with social cognition deficits in patients with FTD.<sup>52,57</sup> Lobule VI, Crus I, and Crus II affected in TDP-C have been associated with language deficits in svPPA.<sup>10,18,54</sup> Crus I and Crus II involved in Pick's have been associated with speech production problems in non-fluent variant PPA (nfvPPA).<sup>10,18,54</sup> Lobules I–VI, Crus I, and the vermis affected in CBD pathology have been associated with abnormal eye movements, hyperreflexia, speech changes, and cognitive deficits in patients with CBS.<sup>50,54</sup> Finally, lobules I–IV, VI, Crus I, and the vermis impacted in the PSP pathology group have been associated with phonological changes, ocular motor impairment, and cognitive deficits in patients with PSP.<sup>50,54</sup>

An important question raised by these results is whether cerebellar atrophy across multiple neurodegenerative diseases is simply the result of Wallerian degeneration or pathological deposition directly damaging cerebellar tissue. In addition, the stage of disease likely plays

a critical role in whether the cerebellum is infiltrated by pathology, but studies describing cerebellar pathology early in the disease process are uncommon. The degree to which pathological deposition is likely, particularly at the early disease stages where we observed atrophy, is largely dependent on the pathology in question.

The patterns of pathological infiltration into the cerebellum are diverse; FTLT tauopathies do infiltrate the cerebellum, but AD amyloid beta infiltrates the cerebellum only at the later stage of the disease, whereas TDP-43 inclusions are never found in the cerebellum. In patients with PSP and CBD pathologies, white matter degeneration has been found in the cerebellar peduncles,<sup>58,59</sup> and the degree of demyelination in this subregion correlates with tau burden in PSP.<sup>60</sup> Although cerebellar tau has been seen only in the middle and later stages in PSP (i.e., stage 3 or later in the Kovacs staging schema),<sup>61</sup> the timing of onset of infiltration in CBD has not yet been precisely established.<sup>62</sup> Tau pathology in PSP begins with neuronal tau accumulation in the pallido-nigro-luysian axis and propagates through the cerebro-ponto-cerebellar tract rostrally to neocortical regions and caudally to the cerebellum including the dentate nucleus.<sup>61,63</sup> Cerebellar atrophy in FTLT-tau subgroups, therefore, may reflect both Wallerian degeneration and pathological deposition. The impact of FTLT-TDP pathology on the cerebellum is more complex, however. Although frank TDP-43 pathology has not been found in the cerebellum at any stage of disease,<sup>64,65</sup> increased RNA foci burden, toxic dipeptide protein repeat inclusions,<sup>66</sup> and p62/ubiquitin-positive but TDP-43-negative

neuronal cytoplasmic inclusions<sup>67-70</sup> are all seen in the cerebellum in *C9orf72* repeat expansion-positive FTD/amyotrophic lateral sclerosis. This abundance could create synaptic dysfunction and may contribute to cerebellar neuron loss in *C9*-expansion positive cases of FTLTDP.<sup>66</sup> However, regardless of *C9orf72* status, our results suggest that Wallerian degeneration of the cerebellum may also be occurring in FTLTDP disease as a result of functional and structural disconnection from the cerebrum. Finally, given the diffuse-type amyloid beta deposition found in the molecular layer of the cerebellar cortex in AD,<sup>71</sup> widespread cerebellar atrophy in AD and LBD-AD pathological subgroups may be mediated by both pathological deposition and Wallerian degeneration. The density of cerebellar amyloid beta, however, does not correlate closely with cerebellar atrophy,<sup>9</sup> so the degree to which cerebellar volume loss is related to cerebellar amyloid remains unclear. Future research is warranted to clarify the spatial characteristics and temporal order of neuropathological changes and their relation to cerebellar atrophy in these diseases.

Our study attempted to disentangle the question of the degree to which cerebellar atrophy is related to Wallerian degeneration by directly examining the relationship between cerebellar and cerebral atrophy. We saw that the degree of overall cerebral atrophy positively predicted the degree of cerebellar atrophy in all subtypes, in the same linear relationship observed in healthy controls, suggesting a picture of co-atrophy in the cerebellum and cerebrum. Given the previously established evidence of differential degrees of pathological infiltration among the different pathologies, this suggests that the atrophy in the cerebellum is likely largely a result of loss of cerebral tissue in functionally and structurally connected areas. Therefore, cerebellar atrophy could be driven by diverse pathological mechanisms, and the penalty mechanisms differ across pathological subtypes.

A key finding of this study is that the cerebellum was affected even in the earlier stages of these diseases, contrary to the expectation derived from prior pathological studies that the cerebellum would be affected only in the later stage of the disease.<sup>72,73</sup> All pathologies other than TDP-B cases showed significant volume loss at the early stage (CDR  $\leq 1$ ). Moreover, cerebellar involvement was also observed in the earlier stage (CDR 0–0.5) in at least one pathology belonging to all three larger pathological categories (i.e., AD, FTLTDP, and FTLT-tau). As described earlier, pathological and imaging evidence converge to suggest that cerebellar atrophy in FTLTDP cases may be driven predominantly by Wallerian degeneration. Thus the limited local cerebral atrophy found early in these TDP-B cases may explain the absence of homologous cerebellar atrophy in the earlier clinical stages of TDP-B. More generally, however, these results indicate that cerebellar involvement in most neurodegenerative disorders is more pronounced earlier than previously thought, and thus cerebellar volume has the potential to be an additional imaging biomarker for early disease detection and disease monitoring.

Although this study provided the first detailed examination of cerebellar involvement in pathological subtypes of dementia, many questions warrant further investigation. First, despite recognizing the traditional CDR's limitations in reflecting disease severity in non-AD pathologies,<sup>36</sup> too small a proportion of our autopsy-proven sample

had received an FTLT-CDR during life. Consequently, we used the less-precise CDR to stage our patients. Within any one condition, using a more focal measurement of key symptoms affecting function (e.g., the Progressive Supranuclear Palsy Rating Scale for PSP,<sup>74</sup> the Cortical Basal Ganglia Functional Scale for CBS<sup>75</sup>) might yield a more precise estimate of cerebellar involvement in earlier clinical stages. Second, for the cerebellum to be a useful diagnostic marker in any neurodegenerative syndrome, quantitative evaluation of pathological burden and its association with cerebellar changes, together with longitudinal and individual studies, will be the next logical steps to clarify the course of cerebellar involvement throughout all stages of disease progression. Finally, mapping the patterns of cerebellar and cerebral atrophy onto known intrinsic connectivity networks is warranted to further understand the mechanisms underlying these anatomic changes, although the apparent co-atrophy of cerebellar and cerebral regions poses methodologic obstacles to functional imaging analysis. Future seed-based functional connectivity analysis in healthy brains using foci of cerebellar atrophy observed in patients at earlier clinical stages could establish a more integrated structure–function view of how the cerebellum contributes to specific clinical symptoms in dementia.

In conclusion, this study identified for the first-time pathology-specific profiles of cerebellar atrophy across all the major categories of neurodegenerative diseases, and demonstrated cerebellar involvement at significantly earlier clinical stages than has been recognized previously. Our study further revealed that the degree of cerebral atrophy positively predicted cerebellar atrophy in all subtypes, suggesting that cerebellar volume loss may largely, although not entirely, be secondary to degenerative damage to connected cerebral tissue, rather than due to direct pathological deposition of the cerebellum. These results underscore the potential for structural neuroimaging of the cerebellum to be an additional non-invasive imaging biomarker supporting both differential diagnosis among pathologies and more precise monitoring of disease progression.

## ACKNOWLEDGMENTS

The authors thank the patients and their families for their continued support as well as the assistance of the support staff of our research. The UCSF Neurodegenerative Disease Brain Bank receives support from National Institutes of Health grants P30AG062422, P01AG019724, U01AG057195, and U19AG063911, as well as the Rainwater Charitable Foundation and the Bluefield Project to Cure FTD. Neuroimaging data acquisition of this study was supported by the ARTFL-LEFFTDS Longitudinal Frontotemporal Lobar Degeneration (ALLFTD) Consortium (U19AG063911, funded by the National Institute on Aging and the National Institute of Neurological Diseases and Stroke), the former ARTFL & LEFFTDS Consortia (ARTFL: U54NS092089, funded by the National Institute of Neurological Diseases and Stroke and National Center for Advancing Translational Sciences; LEFFTDS: U01AG045390, funded by the National Institute on Aging and the National Institute of Neurological Diseases and Stroke). In addition, this work was supported by Larry L. Hillblom Foundation grant 2014-A-004-NET and National Institutes of Health grants P50AG023501 and R01AG029577.

**CONFLICT OF INTEREST STATEMENT**

The authors declare no conflicts of interest.

**CONSENT STATEMENT**

The study was approved by the University of California San Francisco (UCSF) Committee on Human Research. All participants were recruited at the Memory and Aging Center (MAC) of UCSF and provided written informed consent or assent in accordance with the Declaration of Helsinki. This study was performed in accordance with the ethical standards as laid down in the 1964 Declaration of Helsinki and its later amendments or comparable ethical standards.

**ORCID**

Yu Chen  <https://orcid.org/0000-0001-5863-7002>

**REFERENCES**

- Ratnavalli E, Brayne C, Dawson K, Hodges JR. The prevalence of frontotemporal dementia. *Neurology*. 2002;58(11):1615-1621.
- Coyle-Gilchrist IT, Dick KM, Patterson K, et al. Prevalence, characteristics, and survival of frontotemporal lobar degeneration syndromes. *Neurology*. 2016;86(18):1736-1743. doi:10.1212/WNL.0000000000002638
- Association As. 2010 Alzheimer's disease facts and figures. *Alzheimer's Dement*. 2010;6(2):158-194.
- Vann Jones SA, O'Brien JT. The prevalence and incidence of dementia with Lewy bodies: a systematic review of population and clinical studies. *Psychol Med*. 2014;44(4):673-683. doi:10.1017/S0033291713000494
- Azevedo FA, Carvalho LR, Grinberg LT, et al. Equal numbers of neuronal and nonneuronal cells make the human brain an isometrically scaled-up primate brain. *J Comp Neurol*. 2009;513(5):532-541. doi:10.1002/cne.21974
- Gellersen HM, Guo CC, O'Callaghan C, Tan RH, Sami S, Hornberger M. Cerebellar atrophy in neurodegeneration—a meta-analysis. *J Neurol Neurosurg Psychiatry*. 2017;88(9):780-788. doi:10.1136/jnnp-2017-315607
- Guo CC, Tan R, Hodges JR, Hu X, Sami S, Hornberger M. Network-selective vulnerability of the human cerebellum to Alzheimer's disease and frontotemporal dementia. *Brain*. 2016;139(Pt 5):1527-1538. doi:10.1093/brain/aww003
- Chen Y, Kumfor F, Landin-Romero R, Irish M, Piguet O. The cerebellum in frontotemporal dementia: a meta-analysis of neuroimaging studies. *Neuropsychol Rev*. 2019;29(4):450-464. doi:10.1007/s11065-019-09414-7
- Jacobs HIL, Hopkins DA, Mayrhofer HC, et al. The cerebellum in Alzheimer's disease: evaluating its role in cognitive decline. *Brain*. 2018;141(1):37-47. doi:10.1093/brain/awx194
- Chen Y, Kumfor F, Landin-Romero R, Irish M, Hodges JR, Piguet O. Cerebellar atrophy and its contribution to cognition in frontotemporal dementias. *Ann Neurol*. 2018;84(1):98-109. doi:10.1002/ana.25271
- Mackenzie IR, Neumann M, Bigio EH, et al. Nomenclature and nosology for neuropathologic subtypes of frontotemporal lobar degeneration: an update. *Acta Neuropathol*. 2010;119(1):1-4. doi:10.1007/s00401-009-0612-2
- Mackenzie IR, Neumann M, Baborie A, et al. A harmonized classification system for FTLT-DTP pathology. *Acta Neuropathol*. 2011;122(1):111-113. doi:10.1007/s00401-011-0845-8
- Lee EB, Porta S, Michael Baer G, et al. Expansion of the classification of FTLT-DTP: distinct pathology associated with rapidly progressive frontotemporal degeneration. *Acta Neuropathol*. 2017;134(1):65-78. doi:10.1007/s00401-017-1679-9
- Chare L, Hodges JR, Leyton CE, et al. New criteria for frontotemporal dementia syndromes: clinical and pathological diagnostic implications. *J Neurol Neurosurg Psychiatry*. 2014;85(8):865-870. doi:10.1136/jnnp-2013-306948
- Kim E-J, Vatsavayi S, Seeley WW. Neuropathology of dementia. *The Behavioral Neurology of Dementia*. Cambridge University Press; 2016:94-122.
- Robinson JL, Lee EB, Xie SX, et al. Neurodegenerative disease concomitant proteinopathies are prevalent, age-related and APOE4-associated. *Brain*. 2018;141(7):2181-2193. doi:10.1093/brain/awy146
- Spina S, La Joie R, Petersen C, et al. Comorbid neuropathological diagnoses in early versus late-onset Alzheimer's disease. *Brain*. 2021;144(7):2186-2198. doi:10.1093/brain/awab099
- Chen Y, Landin-Romero R, Kumfor F, et al. Cerebellar integrity and contributions to cognition in C9orf72-mediated frontotemporal dementia. *Cortex*. 2022;149:73-84. doi:10.1016/j.cortex.2021.12.014
- Rabinovici GD, Seeley WW, Kim EJ, et al. Distinct MRI atrophy patterns in autopsy-proven Alzheimer's disease and frontotemporal lobar degeneration. *Am J Alzheimers Dis Other Dement*. 2008-2007;22(6):474-488. doi:10.1177/1533317507308779
- Boxer AL, Geschwind MD, Belfor N, et al. Patterns of brain atrophy that differentiate corticobasal degeneration syndrome from progressive supranuclear palsy. *Arch Neurol*. 2006;63(1):81-86. doi:10.1001/archneur.63.1.81
- The National Institute on Aging; Reagan Institute Working Group on Diagnostic Criteria for the Neuropathological Assessment of Alzheimer's Disease. Consensus recommendations for the postmortem diagnosis of Alzheimer's disease. *Neurobiol Aging*. 1997;18(Suppl 4):S1-S2.
- McKeith IG, Dickson DW, Lowe J, et al. Diagnosis and management of dementia with Lewy bodies: third report of the DLB Consortium. *Neurology*. 2005;65(12):1863-1872. doi:10.1212/01.wnl.0000187889.17253.b1
- Montine TJ, Phelps CH, Beach TG, et al. National Institute on Aging-Alzheimer's Association guidelines for the neuropathologic assessment of Alzheimer's disease: a practical approach. *Acta Neuropathol*. 2012;123(1):1-11. doi:10.1007/s00401-011-0910-3
- Braak H, Alafuzoff I, Arzberger T, Kretschmar H, Del Tredici K. Staging of Alzheimer disease-associated neurofibrillary pathology using paraffin sections and immunocytochemistry. *Acta Neuropathol*. 2006;112(4):389-404. doi:10.1007/s00401-006-0127-z
- Rascovsky K, Hodges JR, Knopman D, et al. Sensitivity of revised diagnostic criteria for the behavioural variant of frontotemporal dementia. *Brain*. 2011;134(Pt 9):2456-2477. doi:10.1093/brain/awr179
- Gorno-Tempini ML, Hillis AE, Weintraub S, et al. Classification of primary progressive aphasia and its variants. *Neurology*. 2011;76(11):1006-1014. doi:10.1212/WNL.0b013e31821103e6
- Armstrong MJ, Litvan I, Lang AE, et al. Criteria for the diagnosis of corticobasal degeneration. *Neurology*. 2013;80(5):496-503. doi:10.1212/WNL.0b013e31827f0fd1
- Hoglinger GU, Respondek G, Stamelou M, et al. Clinical diagnosis of progressive supranuclear palsy: the movement disorder society criteria. *Mov Disord*. 2017;32(6):853-864. doi:10.1002/mds.26987
- McKhann GM, Knopman DS, Chertkow H, et al. The diagnosis of dementia due to Alzheimer's disease: recommendations from the National Institute on Aging-Alzheimer's Association workgroups on diagnostic guidelines for Alzheimer's disease. *Alzheimer's Dement*. 2011;7(3):263-269. doi:10.1016/j.jalz.2011.03.005
- Brooks BR, Miller RG, Swash M, Munsat TL. El Escorial revisited: revised criteria for the diagnosis of amyotrophic lateral sclerosis. *Amyotroph Lateral Scler Other Motor Neuron Disord*. 2009;1(5):293-299. doi:10.1080/146608200300079536
- McKeith IG, Boeve BF, Dickson DW, et al. Diagnosis and management of dementia with Lewy bodies: fourth consensus report of the

- DLB Consortium. *Neurology*. 2017;89(1):88-100. doi:10.1212/WNL.0000000000004058
32. Albert MS, DeKosky ST, Dickson D, et al. The diagnosis of mild cognitive impairment due to Alzheimer's disease: recommendations from the National Institute on Aging-Alzheimer's Association workgroups on diagnostic guidelines for Alzheimer's disease. *Alzheimer's Dement*. 2011;7(3):270-279. doi:10.1016/j.jalz.2011.03.008
  33. Geschwind MD. Prion Diseases. *Continuum (Minneapolis)*. 2015;21(6 Neuroinfectious Disease):1612-1638. doi:10.1212/CON.0000000000000251
  34. Morris JC. The Clinical Dementia Rating (CDR): current version and scoring rules. *Neurology*. 1993;43(11):2412-2414. doi:10.1212/wnl.43.11.2412-a
  35. Hughes CP, Berg L, Danziger WL, Coben LA, Martin RL. A new clinical scale for the staging of dementia. *Br J Psychiatry*. 1982;140:566-572. doi:10.1192/bjpp.140.6.566
  36. Miyagawa T, Brushaber D, Syrjanen J, et al. Utility of the global CDR((R)) plus NACC FTLD rating and development of scoring rules: data from the ARTFL/LEFFTDS Consortium. *Alzheimer's Dement*. 2020;16(1):106-117. doi:10.1002/alz.12033
  37. Tartaglia MC, Sidhu M, Laluz V, et al. Sporadic corticobasal syndrome due to FTLD-TDP. *Acta Neuropathol*. 2010;119(3):365-374. doi:10.1007/s00401-009-0605-1
  38. Forman MS, Farmer J, Johnson JK, et al. Frontotemporal dementia: clinicopathological correlations. *Ann Neurol*. 2006;59(6):952-962. doi:10.1002/ana.20873
  39. Spina S, Brown JA, Deng J, et al. Neuropathological correlates of structural and functional imaging biomarkers in 4-repeat tauopathies. *Brain*. 2019;142(7):2068-2081. doi:10.1093/brain/awz122
  40. Zhang Y, Schuff N, Ching C, et al. Joint assessment of structural, perfusion, and diffusion MRI in Alzheimer's disease and frontotemporal dementia. *Int J Alzheimers Dis*. 2011;2011:546871. doi:10.4061/2011/546871
  41. Bettcher BM, Wilhelm R, Rigby T, et al. C-reactive protein is related to memory and medial temporal brain volume in older adults. *Brain Behav Immun*. 2012;26(1):103-108. doi:10.1016/j.bbi.2011.07.240
  42. Gorno-Tempini ML, Dronkers NF, Rankin KP, et al. Cognition and anatomy in three variants of primary progressive aphasia. *Ann Neurol*. 2004;55(3):335-346. doi:10.1002/ana.10825
  43. Andersson J, Jenkinson M, Smith S. Non-linear registration, aka Spatial normalisation. FMRIB Technical report TR07JA2. 2007. <http://www.fmrib.ox.ac.uk/analysis/techrep/tr07ja2.pdf>
  44. Andersson J, Jenkinson M, Smith S. Non-linear optimisation. FMRIB Technical report TR07JA1. 2007. <http://www.fmrib.ox.ac.uk/analysis/techrep/tr07ja1.pdf>
  45. Nichols TE, Holmes AP. Nonparametric permutation tests for functional neuroimaging: a primer with examples. *Hum Brain Mapp*. 2002;15(1):1-25.
  46. Diedrichsen J, Zotow E. Surface-based display of volume-averaged cerebellar imaging data. *PLoS One*. 2015;10(7):e0133402. doi:10.1371/journal.pone.0133402
  47. Diedenhofen B, Musch J. cocor: a comprehensive solution for the statistical comparison of correlations. *PLoS One*. 2015;10(3):e0121945. doi:10.1371/journal.pone.0121945
  48. Stone-Romero EF, Anderson LE. Relative power of moderated multiple regression and the comparison of subgroup correlation coefficients for detecting moderating effects. *J Appl Psychol*. 1994;79(3):354.
  49. Dawson JF, Richter AW. Probing three-way interactions in moderated multiple regression: development and application of a slope difference test. *J Appl Psychol*. 2006;91(4):917-926. doi:10.1037/0021-9010.91.4.917
  50. Tse NY, Chen Y, Irish M, et al. Cerebellar contributions to cognition in corticobasal syndrome and progressive supranuclear palsy. *Brain Commun*. 2020;2(2):fcaa194. doi:10.1093/braincomms/fcaa194
  51. Toniolo S, Serra L, Olivito G, Marra C, Bozzali M, Cercignani M. Patterns of cerebellar gray matter atrophy across Alzheimer's disease progression. *Front Cell Neurosci*. 2018;12:430. doi:10.3389/fncel.2018.00430
  52. Habas C, Kamdar N, Nguyen D, et al. Distinct cerebellar contributions to intrinsic connectivity networks. *J Neurosci*. 2009;29(26):8586-8594. doi:10.1523/JNEUROSCI.1868-09.2009
  53. Sang L, Qin W, Liu Y, et al. Resting-state functional connectivity of the vermal and hemispheric subregions of the cerebellum with both the cerebral cortical networks and subcortical structures. *Neuroimage*. 2012;61(4):1213-1225. doi:10.1016/j.neuroimage.2012.04.011
  54. King M, Hernandez-Castillo CR, Poldrack RA, Ivry RB, Diedrichsen J. Functional boundaries in the human cerebellum revealed by a multi-domain task battery. *Nat Neurosci*. 2019;22(8):1371-1378. doi:10.1038/s41593-019-0436-x
  55. Tse NY, Tu S, Chen Y, et al. Schizotypal traits across the amyotrophic lateral sclerosis-frontotemporal dementia spectrum: pathomechanistic insights. *J Neurol*. 2022;269(8):4241-4252. doi:10.1007/s00415-022-11049-3
  56. Devenney E, Landin-Romero R, Irish M, et al. The neural correlates and clinical characteristics of psychosis in the frontotemporal dementia continuum and the C9orf72 expansion. *NeuroImage Clinical*. 2017;13:439-445. doi:10.1016/j.nicl.2016.11.028
  57. Synn A, Mothakunnel A, Kumfor F, et al. Mental states in moving shapes: distinct cortical and subcortical contributions to theory of mind impairments in dementia. *J Alzheimers Dis*. 2018;61(2):521-535. doi:10.3233/JAD-170809
  58. Whitwell JL, Master AV, Avula R, et al. Clinical correlates of white matter tract degeneration in progressive supranuclear palsy. *Arch Neurol*. 2011;68(6):753-760. doi:10.1001/archneurol.2011.107
  59. Vitali P, Migliaccio R, Agosta F, Rosen HJ, Geschwind MD. Neuroimaging in dementia. *Semin Neurol*. 2008;28(4):467-483. doi:10.1055/s-0028-1083695
  60. Ishizawa K, Lin WL, Tiseo P, Honer WG, Davies P, Dickson DW. A qualitative and quantitative study of grumose degeneration in progressive supranuclear palsy. *J Neuropathol Exp Neurol*. 2000;59(6):513-524. doi:10.1093/jnen/59.6.513
  61. Kovacs GG, Lukic MJ, Irwin DJ, et al. Distribution patterns of tau pathology in progressive supranuclear palsy. *Acta Neuropathol*. 2020;140(2):99-119. doi:10.1007/s00401-020-02158-2
  62. Kouri N, Murray ME, Hassan A, et al. Neuropathological features of corticobasal degeneration presenting as corticobasal syndrome or Richardson syndrome. *Brain*. 2011;134(Pt 11):3264-3275. doi:10.1093/brain/awr234
  63. Passamonti L, Vazquez Rodriguez P, Hong YT, et al. 18F-AV-1451 positron emission tomography in Alzheimer's disease and progressive supranuclear palsy. *Brain*. 2017;140(3):781-791. doi:10.1093/brain/aww340
  64. Kawakami I, Arai T, Hasegawa M. The basis of clinicopathological heterogeneity in TDP-43 proteinopathy. *Acta Neuropathol*. 2019;138(5):751-770. doi:10.1007/s00401-019-02077-x
  65. Geser F, Martinez-Lage M, Robinson J, et al. Clinical and pathological continuum of multisystem TDP-43 proteinopathies. *Arch Neurol*. 2009;66(2):180-189. doi:10.1001/archneurol.2008.558
  66. Kaliszewska A, Allison J, Col TT, Shaw C, Arias N. Elucidating the role of cerebellar synaptic dysfunction in C9orf72-ALS/FTD—a systematic review and meta-analysis. *Cerebellum*. 2022;21(4):681-714. doi:10.1007/s12311-021-01320-0
  67. Boeve BF, Boylan KB, Graff-Radford NR, et al. Characterization of frontotemporal dementia and/or amyotrophic lateral sclerosis associated with the GGGGCC repeat expansion in C9ORF72. *Brain*. 2012;135(Pt 3):765-783. doi:10.1093/brain/aws004

68. Simon-Sanchez J, Dopper EG, Cohn-Hokke PE, et al. The clinical and pathological phenotype of C9ORF72 hexanucleotide repeat expansions. *Brain*. 2012;135(Pt 3):723-735. doi:10.1093/brain/awr353
69. Hsiung GY, DeJesus-Hernandez M, Feldman HH, et al. Clinical and pathological features of familial frontotemporal dementia caused by C9ORF72 mutation on chromosome 9p. *Brain*. 2012;135(Pt 3):709-722. doi:10.1093/brain/awr354
70. Mahoney CJ, Beck J, Rohrer JD, et al. Frontotemporal dementia with the C9ORF72 hexanucleotide repeat expansion: clinical, neuroanatomical and neuropathological features. *Brain*. 2012;135(Pt 3):736-750. doi:10.1093/brain/awr361
71. Gentier RJ, Verheijen BM, Zamboni M, et al. Localization of mutant ubiquitin in the brain of a transgenic mouse line with proteasomal inhibition and its validation at specific sites in Alzheimer's disease. *Front Neuroanat*. 2015;9:26. doi:10.3389/fnana.2015.00026
72. Thal DR, Rüb U, Orantes M, Braak H. Phases of A $\beta$ -deposition in the human brain and its relevance for the development of AD. *Neurology*. 2002;58(12):1791-1800.
73. Ling H, Kovacs GG, Vonsattel JP, et al. Astroglipathy predominates the earliest stage of corticobasal degeneration pathology. *Brain*. 2016;139(Pt 12):3237-3252. doi:10.1093/brain/aww256
74. Golbe LI, Ohman-Strickland PA. A clinical rating scale for progressive supranuclear palsy. *Brain*. 2007;130(Pt 6):1552-1565. doi:10.1093/brain/awm032
75. Lang AE, Stebbins GT, Wang P, et al. The Cortical Basal ganglia Functional Scale (CBFS): development and preliminary validation. *Parkinsonism Relat Disord*. 2020;79:121-126. doi:10.1016/j.parkreldis.2020.08.021

#### SUPPORTING INFORMATION

Additional supporting information can be found online in the Supporting Information section at the end of this article.

**How to cite this article:** Chen Y, Spina S, Callahan P, et al. Pathology-specific patterns of cerebellar atrophy in neurodegenerative disorders. *Alzheimer's Dement*. 2024;20:1771-1783. <https://doi.org/10.1002/alz.13551>